nature geoscience

LETTERS

PUBLISHED ONLINE: 20 JUNE 2016 | DOI: 10.1038/NGEO2740

Emerging impact of Greenland meltwater on deepwater formation in the North Atlantic Ocean

Claus W. Böning[1]*, Erik Behrens[1,2], Arne Biastoch[1], Klaus Getzlaff[1] and Jonathan L. Bamber[3]

The Greenland ice sheet has experienced increasing mass loss since the 1990s[1,2]. The enhanced freshwater flux due to both surface melt and outlet glacier discharge is assuming an increasingly important role in the changing freshwater budget of the subarctic Atlantic[3]. The sustained and increasing freshwater fluxes from Greenland to the surface ocean could lead to a suppression of deep winter convection in the Labrador Sea, with potential ramifications for the strength of the Atlantic meridional overturning circulation[4–6]. Here we assess the impact of the increases in the freshwater fluxes, reconstructed with full spatial resolution[3], using a global ocean circulation model with a grid spacing fine enough to capture the small-scale, eddying transport processes in the subpolar North Atlantic. Our simulations suggest that the invasion of meltwater from the West Greenland shelf has initiated a gradual freshening trend at the surface of the Labrador Sea. Although the freshening is still smaller than the variability associated with the episodic 'great salinity anomalies', the accumulation of meltwater may become large enough to progressively dampen the deep winter convection in the coming years. We conclude that the freshwater anomaly has not yet had a significant impact on the Atlantic meridional overturning circulation.

The subpolar North Atlantic (Fig. 1a) plays an important role in the global climate system due to its generation, by deep convection during winter, of North Atlantic Deep Water that feeds the deep limb of the Atlantic meridional overturning circulation (AMOC). Although annual formation rates vary strongly, primarily due to the variability in atmospheric conditions[7–9], a progressive anthropogenic freshening of the surface waters offers the potential for a persistent weakening of convection intensities. Satellite observations, in conjunction with surface mass balance models, provided detailed reconstructions of the non-uniform distribution of Greenland ice-mass trends[2] and the corresponding freshwater discharge into the ocean[3]. The meltwater fluxes show large increasing trends since the mid-1990s, particularly for the southeastern and western portions of the ice sheet, implying major additional sources of freshwater for the subpolar North Atlantic[10]. Importantly, the ice-mass loss has been increasing over time, including the most recent years[11].

The fate of this additional discharge is not well understood because a meltwater-related freshening trend is difficult to distinguish from the strong decadal variability in the subarctic freshwater content[12,13]. According to ref. 3, the cumulative freshwater anomaly from the ice sheet as a whole amounted to 3,200 km^3 by 2010. From ocean observations it is not possible to infer how much of this input has been retained in the subpolar North Atlantic and, in particular, how much of it has been invading the surface waters of the Labrador Sea, where it could impact the winter convection. The spreading of waters off the Greenland shelf is intimately linked to mesoscale (∼10–30 km) ocean transport processes; specifically, the invasion of the interior Labrador Sea by low-salinity waters from the West Greenland Current (WGC) system is governed by mesoscale eddies arising from an instability of the WGC at the steep bathymetry off Cape Desolation[14,15]. The eddy-induced flux is important for the stability of the near-surface waters[16] and effectively confines the deep convection to the southwestern Labrador Sea[17]. Ocean model studies[18,19] with enhanced resolutions of 0.1° confirmed the key role of eddy processes in the oceanic response to freshwater flux perturbations. However, the use of idealized flux scenarios in these studies, with perturbations of 0.1–0.5 Sverdrup (Sv; 1 Sv = 10^6 m^3 s^{-1}), which exceed the present flux anomalies by an order of magnitude, limits our ability to draw conclusions about the impact of the actual acceleration in the Greenland melting.

We have assessed the fate and impact of the spatially non-uniform increase in the freshwater flux from Greenland, using a set of global ocean–sea-ice models with increasing resolution devised to capture the critical eddy processes in the subpolar North Atlantic. In the high-resolution case (Fig. 1a), the global model mesh of 0.25° was refined to 0.05° in the North Atlantic between 32° and 82° N (corresponding to a mesh size of ∼3 km in the Labrador Sea; Supplementary Information 1), providing an improved realism in the simulation of the complex boundary current system[20]. In particular, the model succeeds in generating a wedge of enhanced mesoscale eddy activity in the northeastern Labrador Sea, originating off Cape Desolation (Fig. 1b).

The impact of the increasing Greenland melting trend was determined by comparing a control simulation forced with climatological coastal runoffs (CNTR) to a case (MELT) with a spatially non-uniform, linearly increasing runoff trend of 16.9 km^3 yr^{-2}, following ref. 3, over a 30-year period beginning in 1990 (Fig. 1c). The atmospheric forcing builds on a bulk formulation of air–sea fluxes with prescribed atmospheric data for 1948–2007 developed for global ocean hindcast simulations[21,22]. Although the unknown future forcing precludes a prediction of the inter-annually varying state of the ocean, we seek to assess the future evolution of the individual impact of the meltwater, as given by the difference between MELT and CNTR, by continuing both experiments for a further 12 years with a repeated atmospheric forcing of the year 2007. The freshwater flux anomalies in MELT were extended by extrapolating the present trend[3]. Until the end of this decade the cumulative runoff anomaly amounts to 7,500 km^3.

[1]GEOMAR Helmholtz Centre for Ocean Research Kiel, Düsternbrooker Weg 20, 24105 Kiel, Germany. [2]National Institute for Water and Atmospheric Research, 301 Evans Parade, Hataitai, Wellington 6021, New Zealand. [3]School of Geographical Sciences, University of Bristol, Bristol BS8 1SS, UK.
*e-mail: cboening@geomar.de

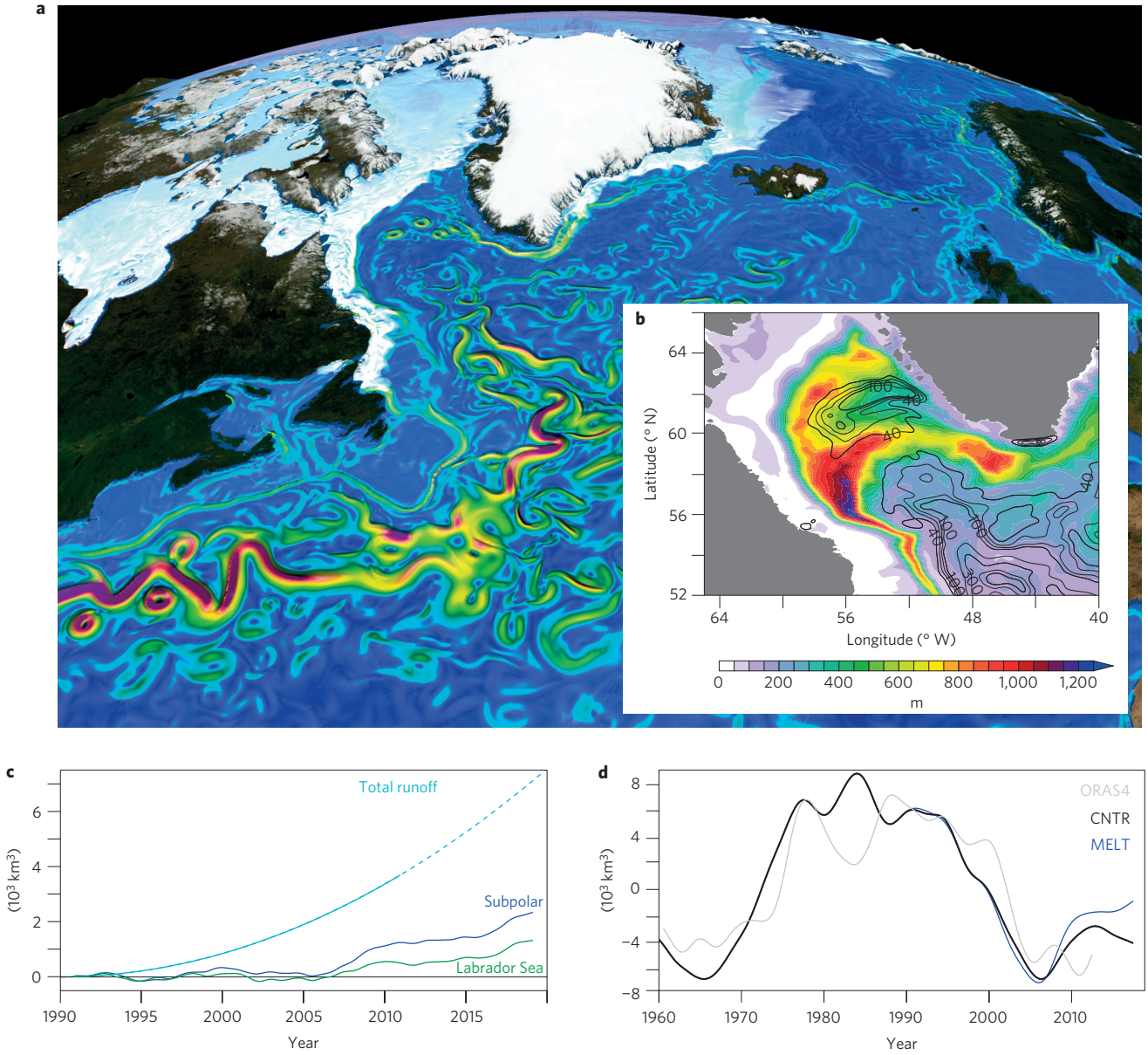

Figure 1 | Circulation and freshwater content of the subpolar North Atlantic. a, Snapshot of surface speed in the high-resolution model illustrating the vigorous eddying currents in the northwestern Atlantic as simulated. **b**, Mean depth of the March mixed layer (colours; in m) and eddy kinetic energy (EKE; contoured); contour interval 25 $cm^2\ s^{-2}$ (100 $cm^2\ s^{-2}$) for EKE below (above) 100 $cm^2\ s^{-2}$. **c**, Cumulated runoff perturbation imposed in MELT using the rate of increase determined by ref. 3 until 2010 (light blue), and its extrapolation through to 2019 (dashed light blue), and the simulated freshwater content anomaly in the subpolar North Atlantic (dark blue), and in the Labrador Sea only (green). **d**, Variability of freshwater content in the upper 2,000 m of the North Atlantic between 50–80° N, derived from the ORAS4 ocean reanalysis data discussed in ref. 30 (grey), and model simulations CNTR (black) and MELT (blue).

However, less than half of the additional meltwater, about 3,000 km^3, is accumulating in the subpolar North Atlantic (Fig. 1c), which represents a relatively small addition to the large decadal changes in the total (0–2,000 m) freshwater content recorded by refs 12,13 (Fig. 1d). We note that the observed decadal variability is captured by the hindcast simulation (CNTR), with a similar freshening trend during the 1970s and 1980s, and its reversal thereafter.

The progression of the meltwater is illustrated by 'dyeing' the additional runoff—that is, by computing the fate of a dye released with the same source distribution as the freshwater off Greenland (Fig. 2 and Supplementary Information 2). In accord with previous studies[18,19,23], highest concentrations are evolving in Baffin Bay, where the runoff from northwest Greenland is superimposed by the northward flow of meltwater by the WGC, and reinforced by a reduction in the southward volume transport through Davis Strait[23,24]. Farther south the spreading in the high-resolution model (Fig. 2a) differs from lower-resolution simulations in two main respects, as emphasized by the companion experiment using the 0.25°-grid without refinement in the North Atlantic (Fig. 2b). First, in the emergence of a near-surface route inshore of the Gulf Stream, providing an outlet for some fraction of the meltwater into the Mid-Atlantic Bight. Second, there are enhanced concentrations over the northern Labrador Sea, owing to the flux by the WGC eddies[10].

A first inference of the potential relevance of the meltwater signal for the convection intensity can be obtained by contrasting the freshwater anomaly developing at present in the surface layer with the historic episodes of surface freshening[25] around 1970 (known

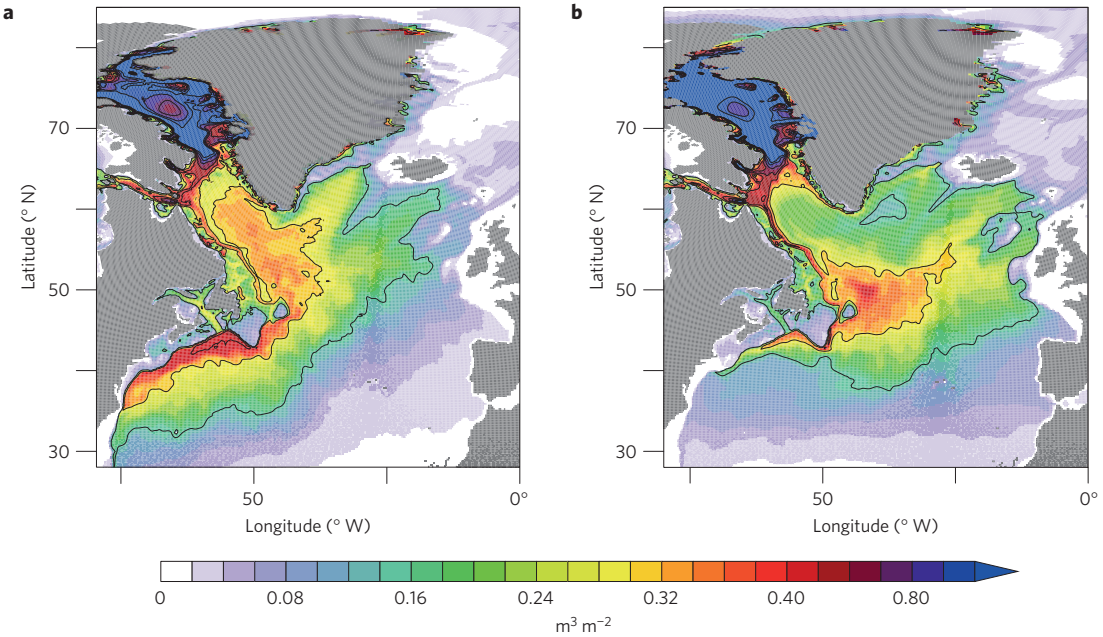

Figure 2 | Fate of the additional Greenland runoff. a,**b**, Distribution of vertically integrated passive tracer content in the last year of MELT in the 0.05° simulation (VIKING20) (**a**) and the 0.25° simulation (ORCA025) (**b**).

as the 'Great Salinity Anomaly', GSA70; ref. 26), the mid-1980s and the early 1990s[27] that were associated with pulses of enhanced sea-ice export from the Arctic Ocean along the shelf of east Greenland[28]. Estimates of the freshwater discharges vary. Pertinent to the consideration here, however, is that the salinity record for the surface layer (0–300 m) of the Labrador Sea suggests[25] that each of these events amounted to a freshwater anomaly of about 1,700 km^3 passing the continental slope region off southwestern Greenland, consistent with an ice export anomaly through Fram Strait of ~2,300 km^3 in the years preceding the GSA70[28]. Our model simulation suggests that the accumulation of meltwater in the Labrador Sea is by now reaching half that magnitude (Fig. 1c).

Meltwater-induced trends in the hydrography of the Labrador Sea occur in a rather gradual way (Fig. 3). Throughout the simulation period, the decrease in the surface salinity remains small compared to the inter-annual variability induced (until 2007) by the atmospheric forcing (Supplementary Information 3). However, the signal is continuously increasing, towards the end of this decade reaching 0.3 in the WGC and 0.1 along the low-salinity wedge extending into the interior Labrador Sea (Fig. 3a,b). To assess the significance of this emerging meltwater signal, it is instructive to contrast the present trend with the surface salinity anomalies occurring during the great salinity anomalies. A manifestation of these events can be seen on the west Greenland shelf, where the salinity in CNTR dropped by about 1 (Supplementary Information 3). The effects in the interior Labrador Sea were smaller, as shown by the record of the GSA70 by former Ocean Weather Ship Bravo (OWS-B)[8]. Its manifestation is also present in the model hindcast. Clearly, the emerging salinity tendencies in MELT are still small compared to these strong, intermittent freshening pulses.

Although not yet of an amplitude comparable to these episodic events, the sustained accumulation of meltwater may have begun to increase the near-surface stability enough to leave a first trace in the intensity of the wintertime convection. Note that the great salinity anomalies, in spite of their similar magnitudes, had considerably different impacts on the convection intensity[29]: whereas the GSA70, in conjunction with a series of mild winters, effectively shut down deep convection for three consecutive years[8,9], there was no obvious impact of the last anomaly during the phase of harsh winters with very strong convection in the early 1990s. Although we cannot predict the absolute year-to-year evolution of convection in the future (nor hindcast inter-annual variations beyond 2007), the difference between MELT and CNTR does provide a useful means of isolating the meltwater impact (Fig. 3c and Supplementary Information 4). Apart from a strong year-to-year variability, primarily reflecting the surface heat loss during winter governed by the imposed atmospheric state, the main signal is the inter-decadal increase from the weak-convection period during the late 1960s and 1970s to a period with maximum intensity during the late 1980s and early 1990s, and its subsequent slackening, in general accordance with previous accounts[29]. Compared to this strong background variability, the effect of the additional meltwater has remained negligible until now. However, it progressively increases during the next years to nearly 30% of the range of variability experienced during the previous decades. We note that the meltwater mainly affects the formation of the dense class of Labrador Sea Water (LSW) in the Labrador Sea, not the lighter, 'upper' LSW formed also in the Irminger Sea (Supplementary Information 4). A corresponding decline is seen in the depth of winter convection, which towards the end of the decade will be reduced by 200–500 m (Fig. 3d). The strongest signals occur along the main meltwater pathways: along the offshore edge of the western boundary current off the Labrador continental slope, and in the interior northern Labrador Sea along the path of the WGC eddies.

With an impact on the intensity of convection not emerging before the end of the decade, we cannot yet expect a significant dynamical repercussion of the increased runoff. Accordingly, there is only a first hint of a weak, but meridionally coherent signal in the AMOC transport emerging towards the end of the simulation period in the MELT–CNTR difference (Supplementary Information 4). This contrasts with the effect of an idealized freshwater perturbation of larger magnitude. As demonstrated in a sensitivity experiment (I-MELT), an instant increase to a constant flux of 3,000 $km^3\ yr^{-1}$ (about 0.1 Sv) leads to a rapid dilution of the surface waters (Supplementary Information 5), a cessation of deep convection after six to eight years, followed by a rapid slowdown of the AMOC by more than 5 Sv. At that point the

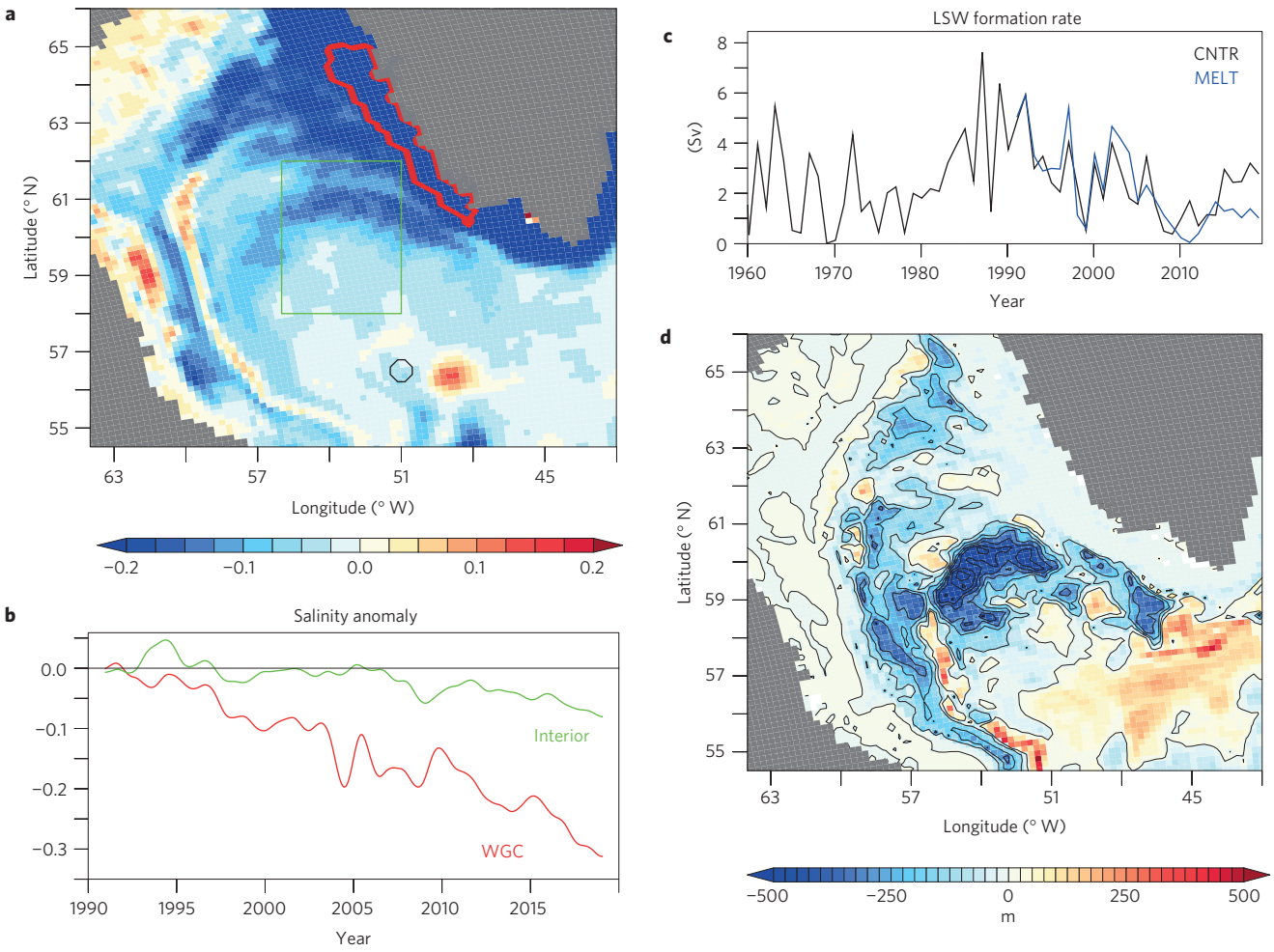

Figure 3 | Trends in Labrador Sea surface salinity and convection intensity. a, Sea surface salinity anomaly in the last year of MELT, the black box indicates the site of OWS-B (see Supplementary Information). **b**, Meltwater-induced trends in sea surface salinity in the WGC (red outline in **a**) and basin interior (green box in **a**) as given by the difference between MELT and CNTR. **c**, Annual formation rate of Labrador Sea Water (LSW), as given by the increase in the volume of the LSW density layer in the Labrador Sea during the winter convection seasons, for CNTR (black) and MELT (blue). **d**, Deviation of March mixed layer depths in MELT from CNTR (average over years 2017–2019), in m.

accumulated runoff exceeds ~20,000 km^3. Under a continuation of the actual observed trend such a magnitude would be reached around 2040. This has some bearing on the hypothesis[6] that the increase in the ice-mass loss from Greenland could already have begun to reduce the AMOC during the second half of the twentieth century. On the basis of the present simulations we argue that the accumulation of meltwater has not been large enough yet to affect the freshwater budget of the subpolar North Atlantic, precluding a significant impact on the AMOC. Another corollary of our simulations is, however, that the ongoing, and perhaps, accelerating melting-induced freshening of the surface waters in the subpolar North Atlantic may begin to progressively affect the deep water formation, and in turn the AMOC, before clear signals of trends in critical hydrographic properties become identifiable, given the strong inter-annual variability in many of these fields.

Methods

Methods, including statements of data availability and any associated accession codes and references, are available in the online version of this paper.

Received 18 December 2015; accepted 17 May 2016; published online 20 June 2016

References

1. Chen, J. L., Wilson, C. R. & Tapley, B. D. Satellite gravity measurements confirm accelerated melting of Greenland ice sheet. *Science* **313,** 1958–1960 (2006).
2. Sasgen, I. *et al*. Timing and origin of recent regional ice-mass loss in Greenland. *Earth Planet. Sci. Lett.* **333–334,** 293–303 (2012).
3. Bamber, J., van den Broeke, M., Etterna, J., Lenaerts, J. & Rignot, E. Recent large increases in freshwater fluxes from Greenland into the North Atlantic. *Geophys. Res. Lett.* **39,** L19501 (2012).
4. Stouffer, R. J. *et al*. Investigating the causes of the response of the thermohaline circulation to past and future climate changes. *J. Clim.* **19,** 1365–1387 (2006).
5. Swingedouw, D. *et al*. Decadal fingerprints of freshwater discharge around Greenland in a multi-model ensemble. *Clim. Dynam.* **41,** 695–720 (2013).
6. Rahmstorf, S. *et al*. Exceptional twentieth-century slowdown in Atlantic Ocean overturning circulation. *Nature Clim. Change* **5,** 475–480 (2015).
7. Kuhlbrodt, T., Titz, S., Feudel, U. & Rahmstorf, S. A simple model of seasonal open ocean convection. Part II: Labrador Sea stability and stochastic forcing. *Ocean Dynam.* **52,** 36–49 (2001).
8. Lazier, J. R. N. Oceanographic conditions at Ocean Weather Ship Bravo, 1964–1974. *Atmos.-Ocean* **18,** 227–238 (1980).
9. Gelderloos, R., Straneo, F. & Katsman, C. A. Mechanisms behind the temporary shutdown of deep convection in the Labrador Sea: lessons from the Great Salinity Anomaly years 1968–71. *J. Clim.* **25,** 6743–6755 (2012).
10. Luo, H. *et al*. Oceanic transport of surface meltwater from the southern Greenland ice sheet. *Nature Geosci.* http://dx.doi.org/10.1038/ngeo2708 (2016).
11. Helm, V., Humbert, A. & Miller, H. Elevation and elevation change of Greenland and Antarctica derived from CryoSat-2. *Cryosphere* **8,** 1539–1559 (2014).

12. Curry, R. & Mauritzen, C. Dilution of the northern North Atlantic Ocean in recent decades. *Science* **308,** 1772–1774 (2005).
13. Boyer, T. *et al*. Changes in freshwater content in the North Atlantic Ocean 1955–2006. *Geophys. Res. Lett.* **34,** L16603 (2007).
14. Prater, M. D. Eddies in the Labrador Sea as observed by profiling RAFOS floats and remote sensing. *J. Phys. Oceanogr.* **32,** 411–427 (2002).
15. Lilly, J. M. *et al*. Observations of the Labrador Sea eddy field. *Prog. Oceanogr.* **59,** 75–176 (2003).
16. Katsman, C. A., Spall, M. A. & Pickart, R. S. Boundary current eddies and their role in the restratification of the Labrador Sea. *J. Phys. Oceanogr.* **34,** 1967–1983 (2004).
17. Kawasaki, T. & Hasumi, H. Effect of freshwater from the West Greenland Current on the winter deep convection in the Labrador Sea. *Ocean Model.* **75,** 51–64 (2014).
18. Weijer, W., Maltrud, M. E., Hecht, M. W., Dijkstra, H. A. & Kliphuis, M. A. Response of the Atlantic Ocean circulation to Greenland ice sheet melting in a strongly-eddying ocean model. *Geophys. Res. Lett.* **39,** L09606 (2012).
19. Toom, M. Den *et al*. Response of a strongly eddying global ocean to North Atlantic freshwater perturbations. *J. Phys. Oceanogr.* **44,** 464–481 (2014).
20. Mertens, C. *et al*. Circulation and transports in the Newfoundland Basin, western subpolar North Atlantic. *J. Geophys. Res. Oceans* **119,** 7772–7793 (2014).
21. Large, W. & Yeager, S. The global climatology of an interannually varying air–sea flux data set. *Clim. Dynam.* **33,** 341–364 (2009).
22. Griffies, S. M. *et al*. Coordinated Ocean-ice Reference Experiments (COREs). *Ocean Model.* **26,** 1–46 (2009).
23. Marsh, R. *et al*. Short-term impacts of enhanced Greenland freshwater fluxes in an eddy-permitting ocean model. *Ocean Sci.* **6,** 749–760.
24. Castro de la Guardia, L., Hu, X. & Myers, P. G. Potential positive feedback between Greenland ice sheet melt and Baffin Bay heat content on the west Greenland shelf. *Geophys. Res. Lett.* **42,** 4922–4930 (2015).
25. Houghton, R. W. & Visbeck, M. H. Quasi-decadal salinity fluctuations in the Labrador Sea. *J. Phys. Oceanogr.* **32,** 687–701 (2002).
26. Dickson, R. R., Meincke, J., Malmberg, S. & Lee, A. J. The "Great Salinity Anomaly" in the northern North Atlantic 1968–1982. *Prog. Oceanogr.* **20,** 103–151 (1988).
27. Belkin, I. M., Levitus, S., Antonov, J. & Malmberg, S.-A. "Great salinity anomalies" in the North Atlantic. *Prog. Oceanogr.* **41,** 1–68 (1998).
28. Vinje, T. Fram Strait ice fluxes and atmospheric circulation: 1950–2000. *J. Clim.* **14,** 3508–3516 (2001).
29. Haine, T. *et al*. in *Arctic-Subarctic Ocean Fluxes* (eds Dickson, R. R., Meincke, J. & Rhines, P.) 653–701 (Springer, 2008).
30. Balmaseda, M. A., Morgensen, K. & Weaver, A. T. Evaluation of the ECMWF ocean reanalysis system ORAS4. *Q. J. R. Meteorol. Soc.* **139,** 1132–1161 (2013).

Acknowledgements

The model computations were performed at the North-German Supercomputing Alliance (HLRN). The study was supported by the cooperative programme 'RACE—Regional Atlantic Circulation and Global Change' (BMBF grant 03F0651B), and the Cluster of Excellence 'The Future Ocean' funded by the DFG. The authors wish to thank the DRAKKAR group for their continuous support in the model development.

Author contributions

All authors conceived the experiments. E.B. implemented the model and performed the experiments. E.B., C.W.B., K.G. and A.B. analysed the results. C.W.B. wrote the paper with contributions by all co-authors.

Additional information

Supplementary information is available in the online version of the paper. Reprints and permissions information is available online at www.nature.com/reprints. Correspondence and requests for materials should be addressed to C.W.B.

Competing financial interests

The authors declare no competing financial interests.

Methods

The numerical models are based on the Nucleus for European Modelling of the Ocean (NEMO) system[31], with some additional modifications of the code and input data as accomplished by the DRAKKAR collaboration[32]. The global ocean models are coupled to the viscous–plastic sea-ice model Louvain-la-Neuve Ice Model (LIM2)[33]. For the turbulent vertical mixing a 1.5-level turbulent kinetic energy (TKE) scheme is applied[34]. Vertical mixing in the case of hydrostatic instability is parameterized by an enhanced vertical diffusion for tracer and momentum.

The high-resolution VIKING20 builds on the widely used eddy-permitting (0.25° horizontal grid) global ocean–sea-ice configuration (ORCA025)[35] by way of a two-way nesting scheme, Adaptive Grid Refinement in FORTRAN (AGRIF)[36], using a grid refinement by a factor of five between 32° and ∼85° N. Although the horizontal mesh size of ORCA025, about 15 km in the Labrador Sea, is not sufficient to capture mesoscale eddy processes governed by the Rossby radii of about 10 km in that region, the high-resolution nest does by resolving the horizontal with mesh sizes of 2–3 km around Greenland (Supplementary Fig. 1a). Both models use 46 z-levels in the vertical, with a partial cell formulation for the lowermost grid boxes[36]. The bathymetry in both cases is based on the same ETOPO (http://www.earthmodels.org/data-and-tools/topography/etopo) and GEBCO (http://www.gebco.net) products; the discretized topographies differ due to the more realistic depiction of steep slopes in the high-resolution case.

The atmospheric forcing uses the bulk formulations and data products for the period 1948–2007 developed in ref. 21 for the Co-ordinated Ocean-ice Reference Experiments (CORE2)[22]. Data were prescribed as six-hourly (wind speed, humidity and atmospheric temperature), daily (short- and long-wave radiation) and monthly (rain and snow) resolution. Following a 30-year spin-up, the control simulation (CNTR) covered the period 1948–2019 by using the inter-annual CORE forcing through 2007, followed by a repetitive application of the year-2007 forcing.

The perturbation experiment (MELT) started from the CNTR-state in 1990, with the same forcing as CNTR, except for the Greenland runoff: the seasonally varying freshwater fluxes entering the ocean grid cells around Greenland were augmented by the regionally differentiated linear trends for 1992–2010 reported by ref. 3 (Supplementary Fig. 1b); the flux anomalies were extended through 2019 by extrapolating the observed trend. This additional discharge is comprised of three components: tundra snowmelt, ice sheet surface melt and solid ice discharge across the grounding line. The first two are seasonally varying, whereas the latter is assumed to be seasonally invariant. Although this assumption is supported by results from the GRACE mission for grounding line discharge, calving fluxes and sub-shelf melting do vary seasonally. We note, however, that 84% of the increase in freshwater flux since 2009 is due to surface melting[37]. In our study, the freshwater fluxes enter the ocean in the first 6-m-thick grid box, although we note that some fraction is also transported close to the polar water/subtropical water boundary[38].

The additional discharge has an increasing trend of 0.52 mSv yr^{-1} (equivalent to 16.9 km^3 yr^{-2}), corresponding to a total flux anomaly of 16.43 mSv by 2019. To avoid an excessive, spurious loss of the runoff anomaly (as noted, for example, in a previous model study[23]), the experiments depart from common practice in global ocean modelling[22] by employing only a very weak damping of sea surface salinity to climatological values with a piston velocity of 16.4 mm d^{-1}, corresponding to a relaxation timescale of 365 days for the 6-m surface level; the damping fluxes were further limited to a maximum salinity change of 0.5, and no damping was applied for a swath around Greenland and in ice-covered regions. The freshening of the surface layer in MELT induces an increase of the damping flux over the North Atlantic and Arctic oceans—that is, an artificial loss of freshwater, of a magnitude which corresponds to about 3–4% of the runoff anomaly: accordingly, the cumulative runoff anomaly of 7,500 km^3 until the end of the decade (Fig. 1c) becomes artificially curbed by ∼250 km^3 (Supplementary Fig. 1c).

A further experiment (I-MELT) considered the effect of a sudden, step-function increase of the runoff to a constant flux of 0.1 Sv (3,100 km^3 yr^{-1}) over a period of 43 years (1965–2007). The role of mesoscale eddy transports was assessed by comparing the VIKING20 simulations with the 0.25° simulations of the base model (ORCA025). For more technical details of the model configurations and experimental set-ups we refer to E. Behrens, The oceanic response to Greenland melting: the effect of increasing model resolution, at http://macau.uni-kiel.de/receive/dissertation_diss_00013684.

Code availability. NEMO is available at http://www.nemo-ocean.eu. The specific additions for generating the model configurations used here can be provided on request.

Data availability. The derived data used for the figures are available at http://data.geomar.de. Model raw data can be provided on request.

References

31. Madec, G. and the NEMO team. *NEMO Ocean Engine* (Institut Pierre-Simon Laplace No. 27, 2008).
32. Barnier, B. *et al*. DRAKKAR: Developing high resolution ocean components for European Earth system models. *CLIVAR Exchanges* **19,** 18–21 (2014).
33. Fichefet, T. & Morales Maqueda, M. A. Sensitivity of a global sea ice model to the treatment of ice thermodynamics and dynamics. *J. Geophys. Res.* **102,** 12609–12646 (1997).
34. Blanke, B. & Delecluse, P. Variability of the tropical Atlantic Ocean simulated by a general circulation model with two different mixed-layer physics. *J. Phys. Oceanogr.* **23,** 1363–1388 (1993).
35. Barnier, B. *et al*. Impact of partial steps and momentum advection schemes in a global ocean circulation model at eddy-permitting resolution. *Ocean Dynam.* **56,** 543–567 (2006).
36. Debreu, L., Vouland, C. & Blayo, E. AGRIF: Adaptive grid refinement in FORTRAN. *Comp. Geosci.* **34,** 8–13 (2008).
37. Enderlin, E. M. *et al*. An improved mass budget for the Greenland ice sheet. *Geophys. Res. Lett.* **41,** 866–872 (2014).
38. Straneo, F. *et al*. Impact of fjord dynamics and glacial runoff on the circulation near Helheim Glacier. *Nature Geosci.* **4,** 322–327 (2011).